How to cite: *Angew. Chem. Int. Ed.* **2024**, *63*, e202318421
doi.org/10.1002/anie.202318421

VIP Microgels Very Important Paper

Local Water Content in Polymer Gels Measured with Super-Resolved Fluorescence Lifetime Imaging

*Sankar Jana, Oleksii Nevskyi, Hannah Höche, Leon Trottenberg, Eric Siemes, Jörg Enderlein, Alexandre Fürstenberg, and Dominik Wöll**

Abstract: Water molecules play an important role in the structure, function, and dynamics of (bio-) materials. A direct access to the number of water molecules in nanoscopic volumes can thus give new molecular insights into materials and allow for fine-tuning their properties in sophisticated applications. The determination of the local water content has become possible by the finding that H_2O quenches the fluorescence of red-emitting dyes. Since deuterated water, D_2O, does not induce significant fluorescence quenching, fluorescence lifetime measurements performed in different H_2O/D_2O-ratios yield the local water concentration. We combined this effect with the recently developed fluorescence lifetime single molecule localization microscopy imaging (FL-SMLM) in order to nanoscopically determine the local water content in microgels, i.e. soft hydrogel particles consisting of a cross-linked polymer swollen in water. The change in water content of thermo-responsive microgels when changing from their swollen state at room temperature to a collapsed state at elevated temperature could be analyzed. A clear decrease in water content was found that was, to our surprise, rather uniform throughout the entire microgel volume. Only a slightly higher water content around the dye was found in the periphery with respect to the center of the swollen microgels.

[*] Dr. S. Jana, H. Höche, L. Trottenberg, E. Siemes, Prof. Dr. D. Wöll
Institute of Physical Chemistry, RWTH Aachen University
Landoltweg 2, 52074 Aachen (Germany)
E-mail: woell@pc.rwth-aachen.de

Dr. O. Nevskyi, Prof. Dr. J. Enderlein
Third Institute of Physics – Biophysics, Georg August University
37077 Göttingen (Germany)

Prof. Dr. J. Enderlein
Cluster of Excellence "Multiscale Bioimaging: from Molecular Machines to Networks of Excitable Cells" (MBExC),
Georg August University
37077 Göttingen (Germany)

Dr. A. Fürstenberg
Department of Physical Chemistry and Department of Inorganic and Analytical Chemistry, University of Geneva
1211 Geneva (Switzerland)

Super-resolution microscopy techniques open up new horizons for investigating biological environments by non-invasively achieving lateral and axial resolutions down to the scale of several nanometers[1,2] and even beyond.[3] While the earlier super-resolution studies have focused on improving spatial resolution, newer research tries to go beyond and obtain additional information such as spectra[4–6] and fluorescence lifetimes. The Enderlein research group developed a fluorescence lifetime single molecule localization super-resolution technique,[7–10] which has recently been applied to biological samples.[11,12] This provides a powerful tool to monitor and investigate nanoscopic heterogeneous environments and properties such as the local polarity using solvatochromic probes,[13] viscosity,[14] and local temperature.[15,16] In addition, it opens up the possibility to address the local water content around suitable dyes in any biological nanoenvironment, since Maillard et al. reported water to be a fluorescence quencher for red-emitting dyes.[17] Direct quantification of the water content inside biological and biocompatible systems is essential not only for a basic understanding[18–20] but also for important applications such as drug design[21] and delivery.

Hydrogels and micro- or nanogels, i.e. particulate hydrogels, are three-dimensional, cross-linked networks of water-soluble polymers.[22] They exhibit high potential for drug delivery[23,24] (also for poorly water-soluble drugs),[25] and clinical applications,[26] bioimaging,[27,28] tissue engineering,[29] uptake, transport, and release of drugs,[30] guestmolecules,[31] and (bio-) molecules, (bio-) catalysis,[32] sensors,[33] photonic materials, or responsive membranes.[34] In several of these applications, microgels are utilized that undergo a volume phase transition[35] between a swollen (hydrated) and a collapsed (dehydrated) state in response to external stimuli (temperature, pH, light, etc.). Super-resolution fluorescence microscopy methods have proven to be suitable for investigating the structure,[36,37] deformation,[38–40] and cross-linking[41,42] of microgels.[43,44] Also, the local polarity could be studied with super-resolution.[45]

Here, for the first time, we utilize super-resolution fluorescence microscopy to investigate local water content. Specifically, super-resolved, localization-based fluorescence lifetime (FLIM) imaging was performed in poly(*N*-isopropylacrylamide) (PNIPAM) microgels. The fluorescence lifetime of the covalently embedded dye ATTO 655 depends on the amount of surrounding water molecules, which act as fluorescence quenchers (see Figure 1).[17,46] Thus, the water content could be estimated by a systematic variation of the

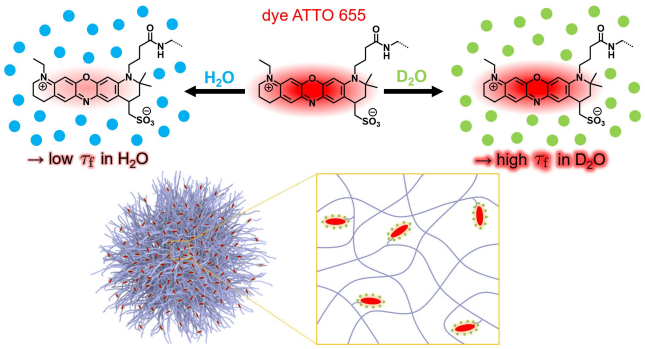

Figure 1. Scheme of fluorescence quenching of ATTO 655 dye in H_2O and restoration of its fluorescence in the presence of D_2O molecules within the first solvation sphere (top). Single microgel particle has been labeled covalently using ATTO 655 dye and measured in aqueous media (bottom).

H_2O/D_2O-solvent ratio and subsequent Stern–Volmer analysis. A significant difference was found between the swollen state at 22 °C, i.e. below the volume phase transition temperature (VPTT[47,48]) of the microgels and their collapsed state at a temperature of 40 °C. Additionally, the super-resolved FLIM approach allowed us to analyze how the water content changed from the center of the microgels towards the periphery. We found a slight, but significant increase in water content in the swollen state, whereas the water content in the collapsed state did not depend on the position within the microgel.

For our studies on water content in microgels, we utilized a thermoresponsive poly(*N*-isopropylacylamide) microgel co-polymerized with *N*-(3-aminopropyl)methacrylamide hydrochloride (P(NIPAM-*co*-APMH)). This microgel displays a volume phase transition (VPT) at approximately 32 °C.[47,48] We covalently labeled the amine groups with the dye ATTO 655 (refer to the Supporting Information for details). We opted for ATTO 655 because its fluorescence lifetime strongly depends on the H_2O content in its direct surroundings.[17] H_2O efficiently reduces its fluorescence lifetime, whereas no noteworthy quenching occurs when it is surrounded by either D_2O or polymer. Further, the dye performs well in super-resolution fluorescence microscopy.

It is well known that PNIPAM microgels swell with water below their VPTT and collapse above this temperature by expelling some of their water. The water content of PNIPAM microgels has been estimated to be approximately 90 % in the swollen state and 70 % in the collapsed state.[49] To compare the swollen and the collapsed states of the microgels, we conducted measurements at four different temperatures, two below (22 °C and 30 °C) and two above (34 °C and 40 °C) the VPTT.

Time-correlated single-photon counting (TCSPC) was employed on a confocal setup with a fast scanner to record FLIM images of P(NIPAM-*co*-APMH) microgels. Super-resolved images were obtained by adding 5 mM cysteamine to the solution to induce blinking, similar to widefield dSTORM. The measurements were taken using a PicoQuant Microtime FLIM setup with a 635 nm excitation laser source, and data was processed using the custom-made Matlab-based TrackNTrace software (for further information, refer to the Supporting Information).[50] Figure 2 depicts the reconstructed FL-SMLM images and corresponding fluorescence lifetime distributions of ATTO 655 dye-labeled P(NIPAM-co-APMH) microgels at 22 °C (on the left) and 40 °C (on the right). Measurements were performed at different H_2O/D_2O-solvent ratios. Figures 2a–c and j–l show selected zoomed-in regions of size 5×5 μm^2 from the reconstructed FL-SMLM images of microgels in pure H_2O. Please find the full-range 10×10 μm^2 images in the Supporting Information (Figures S2 and S3). In the images (a–c and j–l), the different colors represent the local fluorescence lifetime within each pixel, with the scale indicated in the fluorescence lifetime distributions as follows: blue for 2 ns, cyan for 3 ns, orange for 4 ns, and red for 5 ns. Figure 2d–i presents the corresponding fluorescence lifetime distributions, which were histogrammed and average fluorescence lifetimes $\langle \tau_f \rangle$ were calculated from the obtained distributions.

The microgels, appearing as individual point clouds in the FL-SMLM images, exhibit a radius of approximately 320 nm which is comparable to the measured hydrodynamic radius of 256 ± 2 nm obtained from DLS measurement (see the Supporting Information). The average fluorescence lifetimes $\langle \tau_f \rangle$ of ATTO 655 inside the microgels in H_2O are 2.68 ns for 22 °C and 2.92 ns for 40 °C, respectively. With increasing D_2O content, they increase to 3.90 ns and 3.79 ns in pure D_2O, respectively. The values of $\langle \tau_f \rangle$ for different H_2O/D_2O-solvent ratios and at the temperatures considered are listed in Table 1. With the assumption that H_2O quenches the fluorescence of ATTO 655 and its fluorescence lifetime of 1.90 ns in pure water reported by Maillard et al.[17] and also confirmed here, the water content around the dye in the microgels can be estimated as outlined further below. The increased lifetime of ATTO 655 in the H_2O swollen microgels with respect to it being dissolved in pure H_2O can be explained by the presence of polymer around the dye, which replaces H_2O molecules. Such a replacement is unavoidable, at least close to the site of covalent attachment of the dye to the polymer. Another contributing factor would be a restricted mobility of ATTO 655 within the microgel, causing a decrease in the internal conversion (IC) rate constant, as it is known from crowded environments.[51] The hydrogel surrounding in microgels, however, cannot be considered as such a crowded environment. In the D_2O swollen microgels, the average fluorescence lifetime of

Table 1: Average fluorescence lifetimes of ATTO 655-labeled microgels in swollen and collapsed state, respectively, in different D_2O/H_2O solvent mixtures. All lifetime values have an uncertainty of 0.02 ns.

	$\langle \tau_f \rangle$/ns			
$D_2O:H_2O$	22 °C	30 °C	34 °C	40 °C
0:100	2.68	2.64	2.70	2.92
25:75	2.83	2.91	2.96	3.12
50:50	3.22	3.16	3.21	3.36
75:25	3.48	3.47	3.51	3.58
100:0	3.90	3.77	3.71	3.79

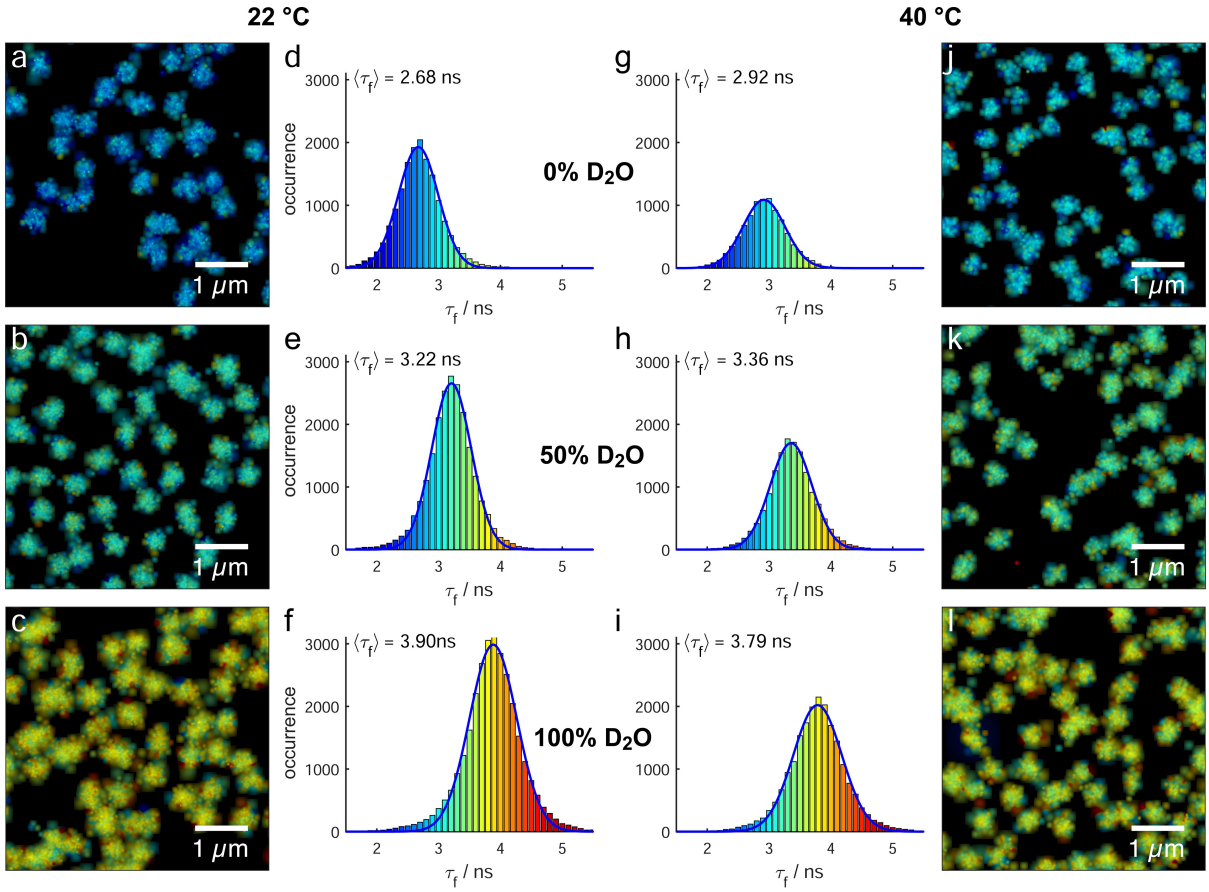

Figure 2. FL-SMLM images and corresponding fluorescence lifetime distributions of microgels at 22 °C (left part of Figure (a–f)) and 40 °C (right part of Figure (g–l) and for three different H_2O/D_2O-ratios (pure H_2O in a, d, g, j; 50% D_2O and 50% H_2O in b, e, h, k; pure D_2O in c, f, i, l), respectively. The FL-SMLM images are intensity-weighted lifetime distributions color-coded in the corresponding fluorescence lifetime. Each point cloud represents a microgel. The same color-code is used for the fluorescence lifetime distribution histograms. The average fluorescence lifetimes $\langle \tau_f \rangle$ are also noted. Extended images and the results for additional H_2O/D_2O-ratios can be found in the Supporting Information.

ATTO 655 (3.90 ns at 22 °C and 3.79 ns at 40 °C) is basically the same as the fluorescence lifetime of 3.9 ns in pure D_2O.[17] The slighter decreased value at 40 °C is not surprising, since the fluorescence lifetimes of dyes at higher temperatures generally decrease. The width of the fluorescence lifetime histograms presented in Figure 2 does not change with an increase in D_2O content or a change in temperature. This allows us to conclude that the polymer network is still not dense enough for the dye to probe significant heterogeneities, even when microgels are in a collapsed state.

Although the fluorescence lifetimes of ATTO 655 within H_2O swollen microgels could provide an estimation of the water content, we aimed to confirm the validity of the Stern–Volmer analysis conducted in solution[17] also for microgels. The well-known Stern–Volmer equation states a linear relationship between the concentration of quencher and the ratio $\frac{\tau_{f,0}}{\tau_f}$ of fluorescence lifetimes without and with quencher:

$$\frac{\tau_{f,0}}{\tau_f} = 1 + k_q \cdot \tau_{f,0} \cdot c_{H_2O} \quad (1)$$

For our purpose of determining the water content around the dye in microgels, we can rewrite the equation as:

$$\frac{\tau_{f,0}}{\tau_f} = 1 + k_q \cdot \tau_{f,0} \cdot c_{H_2O,0} \cdot f_{q,loc} \cdot x_{H_2O} \quad (2)$$

where k_q is the bimolecular rate constant of fluorescence quenching of the dye by H_2O, $c_{H_2O,0}$ is the concentration of H_2O in pure water, x_{H_2O} is the molar fraction of H_2O in the (external) H_2O-D_2O solvent mixture, and $f_{q,loc}$ is the local water content around the dye with respect to the one in pure water solvent.[17] More specifically, $f_{q,loc} = N_{H_2O,loc}/N_{max}$, where $N_{H_2O,loc}$ is the local amount of water molecules in the first solvent shell around the dye and N_{max} is the maximum amount of water molecules as in pure H_2O (for further details see the Supporting Information). In solution, with increasing content of H_2O versus D_2O, fluorescence quenching of the dye through non-radiative energy transfer to higher vibrational harmonics of the H–O stretching vibration of H_2O becomes more dominant.[46] The resulting Stern–Volmer diagram ($\frac{\tau_{f,0}}{\tau_f}$ plotted against x_{H_2O}) exhibits a slope of $0.97 \pm 0.04\ M^{-1}$ for 22 °C (see black dashed line in Figure 3), which does not significantly change when raising

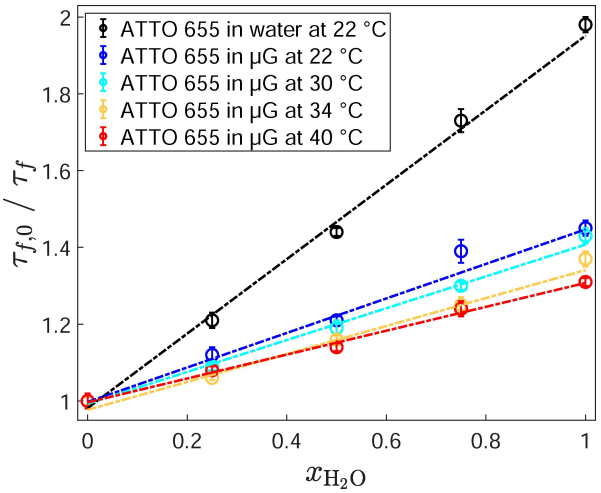

Figure 3. Stern–Volmer plot for fluorescence quenching of ATTO 655 covalently attached to microgels (μG) by surrounding H_2O molecules. The ratio of the fluorescence lifetimes in pure D_2O, $\tau_{f,0}$, and the fluorescence lifetime τ_f at the respective H_2O/D_2O solvent mixture is plotted against the (bulk) molar fraction of water, x_{H_2O}. The data for 22 °C (swollen state), 30 °C (just below the VPTT), 34 °C (just above the VPTT), and 40 °C (collapsed state) are presented in blue, cyan, orange, and red, respectively. The dashed lines are linear fits. For comparison, the Stern–Volmer plot for ATTO 655 in pure water at 22 °C is shown in black. The latter is very similar to the corresponding plot for 40 °C as shown in the Supporting Information.

the temperature to 40 °C (see Figure S6 in the Supporting Information). For dyes embedded in microgels, the slope is flatter because water molecules are replaced by non-quenching polymer in the surrounding of the dye. The slope equals to $0.45 \pm 0.02\ M^{-1}$ at 22 °C, $0.41 \pm 0.02\ M^{-1}$ at 30 °C, $0.36 \pm 0.02\ M^{-1}$ at 34 °C, and $0.31 \pm 0.02\ M^{-1}$ at 40 °C, respectively (see Figure 3).As obvious from Eq. (2), the slope of the Stern–Volmer plot is proportional to the number of water molecules and, thus, to the water content around the dye. This means that 46 %, 42 %, 37 %, and 32 % of the water in the first solvent sphere of the dye in the microgel remains at 22 °C, 30 °C, 34 °C, and 40 °C, respectively, compared with the situation where the dye is free in solution. These values are lower compared to the aforementioned data from the literature. Nerapusri et al. reported for PNIPAM microgels with 1 wt % *N,N'*-methylenediacrylamide (BIS) crosslinker a polymer volume fraction of 20 % in the swollen and 80 % in the collapsed state by analysing refractive indices. With small angle neutron scattering, Stieger et al. found a polymer volume fraction of 13 % below and 42 % above the VPTT for PNIPAM with 5.5 % BIS-crosslinker.[52] For PNIPAM microgels with 8.5 wt % BIS-crosslinker, a decrease of water content from approx. 90 % to approx. 70 % comparing the volume of the dried microgel and after addition of water was estimated by Schmidt et al. using atomic force microscopy (AFM). A nice overview over many studies is presented by Lopez and Richtering who found a polymer volume fraction of 44 % for collapsed microgels independent of crosslinking degree and molar mass.[53] The local water content around the dye measured in our PNIPAM microgel with 5 % crosslinker using the FLIM method is lower than previously reported. We assume that the reason for this is the fact that the dye is covalently linked to the polymer chain and, thus, a part of the volume around it can necessarily not be occupied by water. Also, it should be noted that the energy transfer from a dye to H_2O is only effective at a very short distance which corresponds to the first layer of water molecules around the dye.[46] The ratio between the water fractions in the swollen and collapsed state between the reported "global" (see discussion and citations above) and our "local" (46 % versus 32 %) water content is, however, very similar. Further studies are planned to address how the local water content depends on crosslinking density and on the linker lengths.

None of the methods previously used to determine the water content was able to address whether and how this quantity changes from the center of a microgel to its periphery. Our super-resolution method, however, allows for a determination of the local water content. Since the microgels are basically spheres, we analyzed the radial dependence of water content within single microgels. The fluorescence lifetimes of single ATTO 655 emitters were binned each 20 nm and normalized to their respective value in the center of the microgels (at $r = 0$). They are presented in Figure 4a,b for 22 °C and 40 °C, respectively, and for different H_2O/D_2O-ratios (more details on the distributions of localizations and the non-normalized fluorescence lifetimes can be found in the Supporting Information). The normalized fluorescence lifetime for microgels in their swollen state, at 22 °C, decreases significantly from the center to the periphery as soon as H_2O is present. That means that the water content within the polymer network of the microgels increases with increasing distance from the center. This agrees well with the usual polymer density profile of such swollen microgels with a denser core and a more fluffy periphery. From the fluorescence lifetime changes in the swollen state of the microgels at 22 °C (see Figure S7 in the Supporting Information), we can roughly estimate a lower boundary of 4 % for the change in water content from the center to the periphery. In contrast, no change in fluorescence lifetime was observed for collapsed microgels (see Figure S8 in the Supporting Information), since they can be described as rather homogeneous harder spheres.

In summary, we developed a method for determining the local water content around dye molecules inside polymer gels. For this, we combined the recently developed FL-SMLM imaging technique with a detailed analysis of the quenching of the red-emitting dye ATTO 655 by H_2O. The novel method was used to analyze the local water content inside microgels and to compare the distribution of water in their swollen and collapsed state. On average, a local water content around dyes of 46 % in the swollen and 32 % in the collapsed state was found inside microgels with respect to dyes in pure water. Furthermore, a gradual increase of water content from the center to the periphery of swollen microgels could be observed, whereas such a trend was not found in the collapsed microgels at elevated temperature. Our

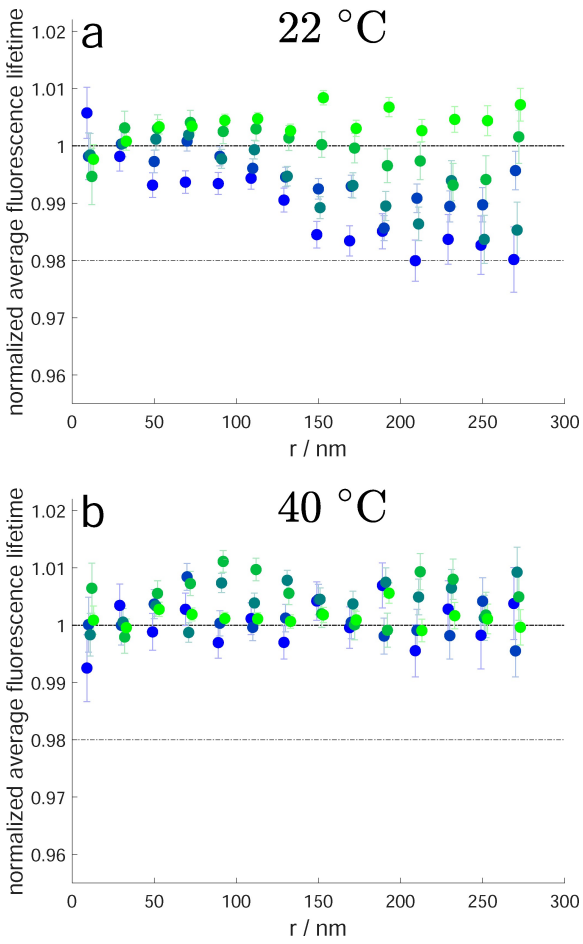

Figure 4. Dependency of fluorescence lifetime on lateral (2D) radial position inside the microgel: radial distribution of fluorescence lifetimes for different H_2O/D_2O solvent mixtures with standard deviation for (a) 22 °C and (b) 40 °C. The color scale from dark blue to light green represents the results for 0%, 25%, 50%, 75%, and 100% D_2O, respectively.

results demonstrate the unprecedented ability of FL-SMLM, in conjunction with water induced quenching of ATTO 655, to nanoscopically measure the local water content around the reporter dyes. Even though we addressed particulate hydrogels in our measurements, the method can be readily transferred to studying other systems or materials, and to applications in the life sciences.

Acknowledgements

We thank the German Research Foundation (Deutsche Forschungsgemeinschaft, DFG) for funding within projects A6 and C5 of the collaborative research centre SFB 985 "Functional microgels and microgel systems". O.N. and J.E. thank the European Research Council (ERC) for financial support via project "smMIET" (grant agreement no. 884488) under the European Union's Horizon 2020 research and innovation program. A.F. acknowledges funding by the Swiss National Science Foundation (project no. 205321_207482). Open Access funding enabled and organized by Projekt DEAL.

Conflict of Interest

The authors declare no conflict of interest.

Data Availability Statement

The data that support the findings of this study are available from the corresponding author upon reasonable request.

Keywords: fluorescence lifetime imaging · fluorescence quenching · hydrogels · microgels · single molecule localization microscopy · super-resolution fluorescence microscopy · water content

[1] M. Bates, J. Keller, A. Przybylski, A. Hüper, T. Stephan, P. Ilgen, A. Cereceda, E. D'Este, A. Egner, S. Jakobs, S. Sahl, S. Hell, *Nat. Methods* **2022**, *19*, 603.
[2] F. Balzarotti, Y. Eilers, K. C. Gwosch, A. H. Gynnå, V. Westphal, F. D. Stefani, J. Elf, S. W. Hell, *Science* **2017**, *355*, 606.
[3] S. Reinhardt, L. Masullo, I. Baudrexel, P. Steen, R. Kowalewski, A. Eklund, S. Strauß, E. Unterauer, T. Schlichthärle, M. Strauss, C. Klein, R. Jungmann, *Nature* **2023**, *617*, 711.
[4] M. N. Bongiovanni, J. Godet, M. H. Horrocks, L. Tosatto, A. R. Carr, D. C. Wirthensohn, R. T. Ranasinghe, J.-E. Lee, A. Ponjavic, J. V. Fritz, C. M. Dobson, D. Klenerman, S. F. Lee, *Nat. Commun.* **2016**, *7*, 13544.
[5] S. Moon, R. Yan, S. J. Kenny, Y. Shyu, L. Xiang, W. Li, K. Xu, *J. Am. Chem. Soc.* **2017**, *139*, 10944.
[6] K.-H. Song, Y. Zhang, G. Wang, C. Sun, H. F. Zhang, *Optica* **2019**, *6*, 709.
[7] J. C. Thiele, M. Jungblut, D. A. Helmerich, R. Tsukanov, A. Chizhik, A. I. Chizhik, M. J. Schnermann, M. Sauer, O. Nevskyi, J. Enderlein, *Sci. Adv.* **2022**, *8*, eabo2506.
[8] N. Oleksiievets, C. Mathew, J. C. Thiele, J. I. Gallea, O. Nevskyi, I. Gregor, A. Weber, R. Tsukanov, J. Enderlein, *Nano Lett.* **2022**, *22*, 6454.
[9] J. C. Thiele, D. A. Helmerich, N. Oleksiievets, R. Tsukanov, E. Butkevich, M. Sauer, O. Nevskyi, J. Enderlein, *ACS Nano* **2020**, *14*, 14190.
[10] N. Oleksiievets, J. C. Thiele, A. Weber, I. Gregor, O. Nevskyi, S. Isbaner, R. Tsukanov, J. Enderlein, *J. Phys. Chem. A* **2020**, *124*, 3494.
[11] D. A. Helmerich, G. Beliu, D. Taban, M. Meub, M. Streit, A. Kuhlemann, S. Doose, M. Sauer, *Nat. Methods* **2022**, *19*, 986.
[12] N. Oleksiievets, Y. Sargsyan, J. C. Thiele, N. Mougios, S. Sograte-Idrissi, O. Nevskyi, I. Gregor, F. Opazo, S. Thoms, J. Enderlein, R. Tsukanov, *Commun. Biol.* **2022**, *5*, 38.
[13] D. I. Danylchuk, S. Moon, K. Xu, A. S. Klymchenko, *Angew. Chem. Int. Ed.* **2019**, *58*, 14920.
[14] X. Peng, Z. Yang, J. Wang, J. Fan, Y. He, F. Song, B. Wang, S. Sun, J. Qu, J. Qi, M. Yan, *J. Am. Chem. Soc.* **2011**, *133*, 6626.
[15] K. Okabe, N. Inada, C. Gota, Y. Harada, T. Funatsu, S. Uchiyama, *Nat. Commun.* **2012**, *3*, 705.
[16] H. Gao, C. Kam, T. Y. Chou, M.-Y. Wu, X. Zhao, S. Chen, *Nanoscale Horiz.* **2020**, *5*, 488.
[17] J. Maillard, C. A. Rumble, A. Fürstenberg, *J. Phys. Chem. B* **2021**, *125*, 9727.

[18] M. Tanaka, T. Hayashi, S. Morita, *Polym. J.* **2013**, *45*, 701.
[19] T. Tsuruta, *J. Biomater. Sci. Polym. Ed.* **2010**, *21*, 1831.
[20] M. L. Samways, R. D. Taylor, H. E. Bruce Macdonald, J. W. Essex, *Chem. Soc. Rev.* **2021**, *50*, 9104.
[21] S. E. Wong, F. C. Lightstone, *Expert Opin. Drug Discovery* **2011**, *6*, 65.
[22] F. A. Plamper, W. Richtering, *Acc. Chem. Res.* **2017**, *50*, 131.
[23] T. R. Hoare, D. S. Kohane, *Polymer* **2008**, *49*, 1993.
[24] X. Peng, Q. Peng, M. Wu, W. Wang, Y. Gao, X. Liu, Y. Sun, D. Yang, Q. Peng, T. Wang, X.-Z. Chen, J. Liu, H. Zhang, H. Zeng, *ACS Appl. Mater. Interfaces* **2023**, *15*, 19560.
[25] R. Dave, G. Randhawa, D. Kim, M. Simpson, T. Hoare, *Mol. Pharm.* **2022**, *19*, 1704.
[26] Y. Kittel, A. J. C. Kuehne, L. De Laporte, *Adv. Healthcare Mater.* **2022**, *11*, 2101989.
[27] Q. M. Zhang, W. Wang, Y.-Q. Su, E. J. M. Hensen, M. J. Serpe, *Chem. Mater.* **2016**, *28*, 259.
[28] X. Zhou, F. Su, Y. Tian, D. R. Meldrum, *PLoS One* **2014**, *9*, e88185.
[29] G. Agrawal, R. Agrawal, *Small* **2018**, *14*, 1801724.
[30] A. S. Hoffman, *Adv. Drug Delivery Rev.* **2002**, *54*, 3.
[31] L. Nuhn, M. Hirsch, B. Krieg, K. Koynov, K. Fischer, M. Schmidt, M. Helm, R. Zentel, *ACS Nano* **2012**, *6*, 2198.
[32] S. Wiese, A. C. Spiess, W. Richtering, *Angew. Chem. Int. Ed.* **2013**, *52*, 576.
[33] S. Su, M. M. Ali, C. D. M. Filipe, Y. Li, R. Pelton, *Biomacromolecules* **2008**, *9*, 935.
[34] D. Menne, F. Pitsch, J. E. Wong, A. Pich, M. Wessling, *Angew. Chem. Int. Ed.* **2014**, *53*, 5706.
[35] G. Del Monte, D. Truzzolillo, F. Camerin, A. Ninarello, E. Chauveau, L. Tavagnacco, N. Gnan, L. Rovigatti, S. Sennato, E. Zaccarelli, *Proc. Natl. Acad. Sci. USA* **2021**, *118*, e2109560118.
[36] A. P. H. Gelissen, A. Oppermann, T. Caumanns, P. Hebbeker, S. K. Turnhoff, R. Tiwari, S. Eisold, U. Simon, Y. Lu, J. Mayer, W. Richtering, A. Walther, D. Wöll, *Nano Lett.* **2016**, *16*, 7295.
[37] P. Otto, S. Bergmann, A. Sandmeyer, M. Dirksen, O. Wrede, T. Hellweg, T. Huser, *Nanosc. Adv.* **2020**, *2*, 323.
[38] G. M. Conley, P. Aebischer, S. Nöjd, P. Schurtenberger, F. Scheffold, *Sci. Adv.* **2017**, *3*, e1700969.
[39] L. Hoppe Alvarez, A. A. Rudov, R. A. Gumerov, P. Lenssen, U. Simon, I. I. Potemkin, D. Wöll, *Phys. Chem. Chem. Phys.* **2021**, *23*, 4927.
[40] X. Shaulli, R. Rivas-Barbosa, M. J. Bergman, C. Zhang, N. Gnan, F. Scheffold, E. Zaccarelli, *ACS Nano* **2023**, *17*, 2067.
[41] E. Siemes, O. Nevskyi, D. Sysoiev, S. K. Turnhoff, A. Oppermann, T. Huhn, W. Richtering, D. Wöll, *Angew. Chem. Int. Ed.* **2018**, *57*, 12280.
[42] A. A. Karanastasis, Y. Zhang, G. S. Kenath, M. D. Lessard, J. Bewersdorf, C. K. Ullal, *Mater. Horiz.* **2018**, *5*, 1130.
[43] O. Nevskyi, D. Wöll, *Annu. Rev. Phys. Chem.* **2023**, *74*, 391.
[44] F. Scheffold, *Nat. Commun.* **2020**, *11*, 4315.
[45] A. Purohit, S. P. Centeno, S. K. Wypysek, W. Richtering, D. Wöll, *Chem. Sci.* **2019**, *10*, 10336.
[46] J. Maillard, K. Klehs, C. Rumble, E. Vauthey, M. Heilemann, A. Fürstenberg, *Chem. Sci.* **2021**, *12*, 1352.
[47] M. Annegarn, M. Dirksen, T. Hellweg, *Polymer* **2021**, *13*, 827.
[48] G. Li, I. Varga, A. Kardos, I. Dobryden, P. M. Claesson, *Langmuir* **2021**, *37*, 1902.
[49] S. Schmidt, M. Zeiser, T. Hellweg, C. Duschl, A. Fery, H. Möhwald, *Adv. Funct. Mater.* **2010**, *20*, 3235.
[50] S. C. Stein, J. Thiart, *Sci. Rep.* **2016**, *6*, 37947.
[51] H. Fidder, M. Rini, E. T. J. Nibbering, *J. Am. Chem. Soc.* **2004**, *126*, 3789.
[52] M. Stieger, W. Richtering, J. S. Pedersen, P. Lindner, *J. Chem. Phys.* **2004**, *120*, 6197.
[53] C. G. Lopez, W. Richtering, *Soft Matter* **2017**, *13*, 8271.

Manuscript received: December 1, 2023
Accepted manuscript online: January 2, 2024
Version of record online: January 29, 2024